

Terra Validation Progress Report

Study: EOS Validation of Aerosol and Water Vapor Profiles by Raman Lidar

Investigators: R. Ferrare, S.H. Melfi, G. Schwemmer, D. Whiteman, K. Evans, D. Turner

Date: May 26, 2000

Contact: Rich Ferrare, MS 401A, NASA Langley Research Center, Hampton, Virginia 23681, 757-864-9443,
r.ferrare@larc.nasa.gov

Abstract

We are developing and using the aerosol extinction and backscattering profiles measured by two Raman lidar systems to validate the aerosol climatology models used by two Terra sensors, MODIS and MISR. The aerosol retrieval algorithms used by these EOS sensors operate by comparing measured radiances with tabulated radiances that have been computed for specific aerosol models. These aerosol models are based almost entirely on surface and/or column averaged measurements and so may not accurately represent the ambient aerosol properties. Therefore, to validate these EOS algorithms, we have developed and are using the aerosol backscattering and extinction profiles measured by the CART Raman Lidar (CARL) to determine how the aerosol properties over the SGP site vary with altitude and time. Additional activities involve the use of the aerosol profiles measured by the GSFC Scanning Raman Lidar (SRL) during periodic field experiments to perform similar assessments. We have begun using these lidar aerosol and water vapor measurements for directly validating these Terra instruments.

SGP CART Raman Lidar Instrument Status:

- During February 1999, laser flashlamps and laser rod were replaced. An uninterruptable power supply (UPS) was installed to keep the system running during frequent brief A/C power interruptions.
- During March 1999, a laser amplifier was replaced.
- System was down during June 1999 and most of July 1999 in order to replace flashlamps, acquire and replace a new laser high voltage wiring harness, and to repair the THG (tripier) crystal. System resumed normal operations in August 1999.
- Upgraded system software for Y2K compliance, repaired damaged laser optics, realigned aft optics, and acquired calibration datasets in September 1999.
- Replaced laser amplifier cladding and realigned beam expander in November 1999.
- Faulty MCS card prevented acquisition of depolarization data during January 2000.
- Installed temperature and humidity sensors inside trailer and installed new picomotor driver in February 2000.
- Between May 1999 and April 2000, CART Raman Lidar operated about 56% of the time. During March and April 2000, and at the present time, the system is running approximately 95% of the time. (**Figure 1**).

3rd Year (5/99-4/00) Objectives

- Continue with routine processing of CART Raman lidar data.
- Continue evaluation of CART Raman lidar aerosol extinction and optical thickness algorithms and retrievals.
- After above evaluations, we shall place the code for all the CART Raman lidar aerosol and water vapor products on the ARM Experiment Center. These algorithms will then run automatically and will place netCDF files of output products at the ARM Archive for public access. We anticipate this to occur by fall, 1999.
- With processing of about 1 year of data complete, we are beginning to examine on statistical basis, properties of aerosol extinction and optical thickness and water vapor and relative humidity profiles derived from CART Raman lidar data. We intend to characterize how the vertical distribution of aerosols varies. We expect this work to carry on through summer and fall, 1999.
- We are presently working with NASA GSFC to develop necessary software and procedures to acquire and work with MODIS aerosol and water vapor data. We plan to have this software in place by the time MODIS level 2 data become available, which is about 60 days after launch.
- We plan to acquire MODIS level 2 aerosol and water vapor data over the ARM CART site on a daily basis, when they become available. Once we acquire these data, we shall then begin comparisons of aerosol optical thickness and precipitable water vapor between the CART Raman lidar and MODIS and MISR to validate these

measurements. We shall also begin to characterize the vertical distribution of aerosol extinction during the MODIS and MISR retrievals. We anticipate that these activities will require several months of coincident Raman lidar and MODIS and MISR measurements to acquire sufficient statistics for meaningful comparisons.

Data Processing Progress/Status:

- A series of Value Added Procedures (VAPs), which we developed to use the CART Raman lidar data to routinely produce several data sets used to characterize the clear-sky state over the SGP site, were implemented to run routinely at the Dept. of Energy Atmospheric Radiation Measurement (ARM) Experiment Center. The output products from these VAPs included a series of netCDF files that include the profile results as well as several quick look GIF images to show the results of this processing. These VAPS include:
 - MR VAP (water vapor mixing ratio and relative humidity profiles)
 - ASR VAP (aerosol scattering ratio and backscatter coefficient profiles)
 - EXT VAP (aerosol extinction coefficient and extinction/backscatter ratio)
 - DEP VAP (depolarization and cloud mask profiles).
- Automated algorithms to derive aerosol scattering ratio, backscattering, and extinction profiles from the SGP CART Raman Lidar data were recently upgraded to improve performance during conditions of low aerosol loading. The corresponding VAPs discussed above were also updated at the ARM Experiment Center.
- These aerosol and water vapor profiles (Raman lidar) and temperature profiles (AERI+GOES) have been combined into a single "best estimate" (BE) VAP that takes advantage of both active and passive remote sensors to characterize the clear sky atmospheric state above the CART site. The products included in this BE VAP are profiles of water vapor mixing ratio, relative humidity, aerosol backscatter coefficient (at 355 nm), aerosol extinction coefficient (at 355 nm), temperature (from AERI+GOES retrievals), potential temperature (from AERI+GOES retrievals), total precipitable water vapor, aerosol optical thickness (at 355 nm), linear depolarization ratio, cloud mask. The characteristics of these products are listed in **Table 1**. This BE VAP has also been implemented to run routinely at the ARM Experiment Center.
- The "best estimate" algorithms have been used to derive profiles for the following periods
 - September 1996 (Water Vapor IOP #1)
 - September-October 1997 (Water Vapor IOP#2, Aerosol IOP)
 - April 1998 through present (May 2000)
- The "best estimate" data have been processed and are available in netCDF form by contacting either Ferrare or Turner or are available from the ARM experiment center. A web site showing these results for the periods listed above has been established at http://yard.arm.gov/~turner/raman_lidar_quicklooks.html. **Figure 2** shows examples of these images for a single day (December 3, 1998).
- We are presently acquiring MODIS level 2 products 04, 05, 06, and 07 as they are processed on the NASA GSFC Windhoek processing computer. We have begun analyzing these data and comparing MODIS results with ARM SGP measurements.

Science Results

Water Vapor, Temperature, and Aerosol Optical Thickness Evaluations

- As part of the routine diagnostics, the CART Raman Lidar (CARL) water vapor mixing ratio profiles were compared with water vapor profiles measured by Vaisala radiosondes launched at the SGP site. Over 500 lidar/radiosonde profile comparisons examined between April 1998 and October 1999 showed that the unscaled radiosondes were about 3-5% drier than the lidar. When the radiosonde water vapor mixing ratio was scaled to match the microwave precipitable water vapor amount, the scaled radiosonde and lidar water vapor profiles agreed generally within 1-2%. **Figure 3** shows these results.
- The AERI+Model temperature profiles were also compared with temperature profiles measured by Vaisala radiosondes. Over 450 AERI+model/radiosonde profile comparisons showed that rms temperature differences were less than 1 K, with the AERI+Model slightly (~0.25 K) warmer. **Figure 4** shows the comparison.
- Aerosol optical thicknesses (AOT), which are computed by integrating the Raman lidar aerosol extinction profiles between 0-6 km, have been compared with simultaneous and independent measurements of AOT made

by a Cimel sun photometer at the SGP CART site (**Figure 5**). The lidar and sun photometer AOT values generally agree, with about a 5% bias difference. Of this difference, 3.5% can be explained by the wavelength dependence of aerosol extinction between the two wavelengths (340 nm vs. 355 nm). The CARL AOT also generally show good agreement with the Cimel AOT when compared as a function of season (**Figure 6**).

Vertical Variability of Aerosols and Water Vapor

- The Raman lidar aerosol extinction, water vapor, and relative humidity profiles have been used to examine the vertical variability of aerosols and water vapor. **Figure 7** shows the average aerosol extinction profiles for various ranges of AOT for data acquired between April 1998 to January 2000. The solid points on this graph indicate the scale height of the aerosols. **Figures 8 and 9** show the same for water vapor mixing ratio and relative humidity. The aerosol scale height was between 1.0-1.2 km during the winter but rose to nearly 2 km in the summer. This behavior is in contrast to the scale height for water vapor mixing ratio, which remained nearly the same (2.0-2.5 km) during winter and summer. (Manuscript submitted to JAM: “Automated retrievals of aerosol extinction and backscatter coefficient profiles from a Raman lidar”, D.D. Turner, R.A. Ferrare, L.A. Heilman, W.F. Feltz, and T. Tooman).
- The CARL aerosol extinction profiles also show that considerable aerosol loading often existed in elevated layer above the boundary layer. **Figure 10** shows an example when smoke from fires in Central America were observed over the ARM SGP CART site. Of particular importance in this case is the profile of the aerosol extinction/backscatter ratio (S_a) derived from the CARL data and which is also shown in this figure. Since S_a varies with changes in the aerosol size distribution and/or aerosol composition, variations in the vertical profile of S_a indicate that the aerosol size distribution and/or aerosol composition varied with altitude. In this example, the value of $S_a = 55$ sr observed for the boundary layer aerosols is typical of the aerosols observed over the SGP site. In contrast, the value of $S_a = 90$ sr observed for the elevated aerosol layer between 3-6 km is typical for biomass burning aerosols. We used aerosol size distributions derived from the Cimel Sun photometer sun and sky radiance measurements to show that the biomass burning aerosols are consistent with the CARL S_a measurements.
- We examined the aerosol extinction/backscattering profiles derived from the CARL measurements to determine the how often aerosol optical and physical characteristics vary with altitude as in the case described above. In this study, we computed the standard deviation (due to atmospheric variability) of S_a in a vertical column. For cases when the AOT at 355 nm was greater than 0.3, **Figure 11** shows that, for data acquired between April 1998 and April 1999, in about 20% of the cases the standard deviation of S_a due to atmospheric variability was greater than 10 sr (or 15%). This type of variability is similar to that shown in **Figure 10** for the smoke aerosols. In these cases of high S_a variability, the aerosol size distribution and/or composition varied significantly with altitude. Since the aerosol parameters derived from the MODIS retrievals represent column averages, this suggests that these column averages may not accurately represent the true aerosol characteristics in a significant number of cases.

Analyses of Aerosol Optical and Physical Characteristics and Relationship with Relative Humidity

- The CARL retrievals of S_a were compared with the aerosol size parameters derived from coincident sun and sky radiance data measured by a Cimel Sun photometer data. An inversion procedure, which has been developed by Oleg Dubovik at NASA/GSFC, uses the Cimel direct solar and the sky brightness measurements to derive column-averaged aerosol size distribution, complex refractive index, and single scattering albedo, as well as the aerosol extinction/backscatter ratio. **Figure 12** shows a comparison of the CARL and Cimel S_a values as well as how these values vary with wavelength. **Figure 13** shows that the CARL S_a values are linearly correlated with the fine (accumulation) mode volume median radius as well as the volume ratio (fine/coarse). This shows that the CARL S_a measurements may be used to indicate particle sizes.
- The CARL data have also been used to investigate how aerosol extinction and the aerosol extinction/backscatter ratio vary with relative humidity. **Figure 14** shows an example of how CARL data have been used to observe the increase in aerosol extinction with relative humidity near the top of the daytime boundary layer. We have examined measurements from several of these days to show the dependence of aerosol extinction and S_a on relative humidity. **Figure 15** shows that the ratio of aerosol extinction at RH=80% to that at RH=30% is about 1.9 +/- 0.4 which is not inconsistent with the values derived from the SGP surface in situ measurements. The

increase in S_a with relative humidity also shown in **Figure 15** is consistent with that modeled for “continental aerosols”.

MODIS Product Validation

- We have presently acquired MODIS level 2 products 04, 05, 06, and 07 since day 57 (Feb 26, 2000) from the NASA GSFC Windhoek computer.
- We have begun comparisons of corrected optical depth land (MOD04), water vapor (IR), and water vapor (near IR) (MOD05) and the corresponding measurements from the ARM SGP sensors. **Figure 16a** shows initial comparisons of aerosol optical thickness (AOT) and **Figure 16b** shows initial comparisons of precipitable water vapor (PWV). These initial comparisons show considerable scatter between the MODIS and Raman lidar measurements. This scatter may be due to cloud contamination of MODIS products, temporal and spatial variability within the comparison location, and incorrect assumptions of the surface albedo around the ARM SGP area. We are continuing to acquire these data and investigate these AOT and PWV differences.

Comparison of SRL measurements and GOES

- Using NASA/GSFC Scanning Raman Lidar (SRL) measurements of cirrus cloud optical depth and water vapor acquired at Andros Island, Bahamas in 1998, we have studied the sensitivity of thin cirrus clouds on GOES retrievals of total precipitable water. A comparison of SRL total precipitable water, GOES retrieved precipitable water and cirrus optical depth is shown in **Figure 17**. (Manuscript submitted to JGR: “Raman lidar measurements of water vapor and cirrus clouds during the passage of hurricane Bonnie”, D.N. Whiteman, K.D. Evans, B. Demoz, D.O’C. Starr, D. Tobin, W. Feltz, G.J. Jedlovec, S.I. Gutman, G. K. Schwemmer, M. Cadirola, S. H. Melfi, F. J. Schmidlin).
- This study concluded that satellites must be able to detect thin cirrus clouds with IR optical depths as low as 0.005 in order to avoid errors in retrieved total precipitable water. These same techniques will be used to compare SRL and MODIS during the WVIOP this fall.

Cirrus Multiple Scattering Calculations and Particle Size Retrieval Algorithm

- The influence of multiple scattering on lidar measurements of cirrus cloud optical depth has been studied. An iterative technique has been developed which allows the multiple scattering component of the signal to be removed. This technique also derives bulk extinction to backscatter ratio as well as the equivalent cirrus particle radius. In this context, equivalent particle radius means the radius of the sphere that has equivalent diffraction properties as the cirrus crystals. An example is shown in **Figure 18**.
- SRL measurements of cirrus clouds were made at GSFC during the Terra overpass on the night of April 13. The MODIS data for this case are not yet available but when the data are available, we will compare lidar derived optical depth to that of MODIS. Additional comparisons between the SRL and MODIS will be made at GSFC in preparation for the deployment at the SGP CART site in September.

Collaborations

- Have been in extensive contact with MODIS atmospheres team (Yoram Kaufman, Lorraine Remer) regarding use of CART Raman lidar data for characterizing vertical distribution of aerosols
- Have been working with Bill Ridgway and Eric Moody (NASA GSFC) in acquiring MODIS data products and in producing a subset of these products over the ARM SGP site.
- Collaborated with Randy Peppler (Univ. of Oklahoma) in multi-sensor study of smoke from Central America fires over CART site. This paper has been accepted for publication by the *Bulletin of the American Meteorological Society*. (see also <http://parker.gcn.ou.edu/~cimms/ARM/smoke.html> and http://www.arm.gov/docs/documents/technical/conf_9903/author.html#P)
- Collaborated with Seiji Kato (Hampton U/NASA LaRC) in comparison of aerosol optical thickness profiles measured by CART Raman lidar and aircraft in situ sensors. This paper was accepted for publication by *Journal of Geophysical Research-Atmospheres*.

- At the second Global Aerosol Climatology Program (GACP) meeting, we gave a presentation explaining the CART Raman lidar aerosol measurements and how these may be used for compiling an aerosol climatology.
- At the request of Dr. Tom Ackerman (DOE ARM Chief Scientist), two of us (Ferrare, Turner) are now co-chairman of the ARM Aerosol Working Group. We are working to coordinate ARM aerosol activities.

Data archival and access

- "Best estimate" data have been processed and are available in netCDF form by contacting either Ferrare or Turner. These data cover the periods: September 1996 (Water Vapor IOP #1), September-October 1997 (Water Vapor IOP#2, Aerosol IOP), and April 1998 through the present (May 2000). A web site showing these results for the periods listed above has been established at http://yard.arm.gov/~turner/raman_lidar_quicklooks.html. We are in the process of placing these files on the ARM archive (<http://www.archive.arm.gov/data/ordering.html>) where they will be available for public access. We anticipate that this will occur by June 2000. Best estimate products are being produced on a routine basis by automated software at the DOE ARM Experiment Center. These data are also available from the ARM Archive.

Web pages

Main validation web page: http://yard.arm.gov/~turner/EOS_validation/

"Best-estimate" quicklook images: http://yard.arm.gov/~turner/raman_lidar_quicklooks.html

Related URL: http://yard.arm.gov/~turner/doe_aerosols.html

FY01 Planned Activities

CART Raman Lidar data processing

- We shall continue with routine processing of CART Raman lidar data and will monitor production of aerosol, water vapor, and best estimate products by ARM Experiment Center.
- We shall continue to evaluate CART Raman lidar aerosol extinction and optical thickness algorithms and retrievals with comparisons with Cimel Sun photometer data and other sensors. We shall extend our analyses of aerosol and water vapor vertical variability and relationship to relate humidity with the data collected on an ongoing basis.

MODIS and MISR data evaluation

- We shall continue acquiring MODIS data on a regular basis. We shall compare MODIS retrievals of aerosol optical thickness (AOT) and precipitable water vapor (PWV) with those derived from ARM SGP Raman lidar (AOT, PWV) and microwave radiometer (PWV). We shall also evaluate how the MODIS retrievals of aerosol Angstrom exponent compare with the CARL retrievals of the aerosol extinction/backscatter ratio.
- We shall begin acquisition of MISR aerosol level 2 data as they become available from the Langley DAAC. We shall compare MISR retrievals of aerosol optical thickness (AOT) with those derived from ARM SGP Raman lidar.
- We shall also begin to characterize the vertical distribution of aerosol extinction and water vapor during the MODIS and MISR retrievals.

NASA/GSFC Scanning Raman Lidar (SRL)

- The SRL will be deployed to the ARM SGP Site to acquire high resolution measurements of water vapor and aerosols as part of the ARM/FIRE Water Vapor IOP Experiment (AFWEX). (This deployment is funded by the DOE.) The high resolution SRL measurements of aerosols and water vapor will be used to directly assess the measurements of MODIS and MISR as well as to assess the low altitude measurement capability of the upward-looking CART Raman lidar.
- Newly implemented aerosol Value Added Procedures (VAPs) using data from the DOE CART Raman lidar, which are a part of the automated data stream generated at the northern Oklahoma CART site, will be tested

using scanned data from the SRL. Assumptions about the vertical distribution of aerosols are made in these routines which can be tested using the data acquired by the SRL.

Presentations

“CART Raman Lidar Retrievals of Aerosol Extinction and Relative Humidity Profiles”, R.A. Ferrare, D.D. Turner, L.A. Heilman, W.F. Feltz, Optical Remote Sensing of the Atmosphere Technical Digest, Optical Society of America, June 22-24, 1999, Santa Barbara, CA, 32-34.

"Characterizing the water vapor profiling measurements at the ARM SGP CART site." D.D. Turner, W.F. Feltz, and W.L. Smith. OSA Optical Remote Sensing of the Atmosphere, Santa Barbara, CA, 22 - 24 June, 1999.

“CART Raman Lidar Retrievals of Aerosol Extinction and Relative Humidity Profiles”, D.D. Turner, R.A. Ferrare, L.A. Heilman, W.F. Feltz, 10th Conference on Atmospheric Radiation, American Meteorological Society, June 28-July 2, 1999, Madison, Wisconsin, 434-437.

"Aerosol Profile Data Sets Derived from Airborne and Ground-Based Lidar Measurements", Richard A. Ferrare, Edward V. Browell, Syed Ismail, William B. Grant, David D. Turner, Tim, GACP Science Team Meeting, New York, NY, September 29-October 1, 1999.

“Raman Lidar Profiling of Water Vapor and Aerosols over the ARM SGP Site”, R.A. Ferrare, D.D. Turner, L.A. Heilman, W.F. Feltz, R.A. Peppler, T. Tooman, and R. Halthore, Symposium on Lidar Atmospheric Monitoring, American Meteorological Society, American Meteorological Society, January 9-14, 2000, 1-4.

“Characterization of the Atmospheric State above the SGP Using Raman Lidar and AERI/GOES Measurements”, R.A. Ferrare, D.D. Turner, L.A. Heilman, W.F. Feltz, T. Tooman, O. Dubovik, R. Halthore, Tenth ARM Science Team Meeting, San Antonio, Texas, March 13-17, 2000, (http://www.arm.gov/docs/documents/technical/conf_0003/ferrare-ra.pdf)

“Study of the Influence of Thin Cirrus Clouds on Satellite Radiances Using Raman Lidar and GOES Data”, D.N. Whiteman, D. O’C Starr, G. Schwemmer, K. D. Evans, B. B. Demoz, M. Cadirola, and S. H. Melfi, G. J. Jedlovec, Tenth ARM Science Team Meeting, San Antonio, Texas, March 13-17, 2000, (http://www.arm.gov/docs/documents/technical/conf_0003/whiteman-dn.pdf)

“Simultaneous Ground-Based Remote Sensing of Water Vapor by Differential Absorption and Raman Lidars”, D. D. Turner, H. Linné, J. Bösenberg, S. Lehmann, K. Ertel, J. E. M. Goldsmith and T. P. Tooman, Tenth ARM Science Team Meeting, San Antonio, Texas, March 13-17, 2000, (http://www.arm.gov/docs/documents/technical/conf_0003/turner-dd.pdf)

Publications

Ferrare, R.A., D.D. Turner, L.A. Heilman, O. Dubovik, and W. Feltz, Raman lidar measurements of the aerosol extinction/backscatter ratio, (in preparation).

Kato, S., M.H. Bergin, T.P. Ackerman, T.P. Charlock, E.E. Clothiaux, R.A. Ferrare, R.N. Halthore, N. Laulainen, G.G. Mace, J. Michalsky, and D.D. Turner, A comparison of the aerosol optical thickness derived from ground-based and airborne measurements”, *J. Geophys. Res.*, in press, 2000.

Peppler, R.A., C.P. Bahrmann, J.C. Barnard, J.R. Campbell, M.-D. Cheng, R.A. Ferrare, R.N. Halthore, L.A. Heilman, D.L. Hlavka, N.S. Laulainen, C.-J. Lin, J.A. Ogren, M.R. Poellot, L.A. Remer, K. Sassen, J.D.

Spinhirne, M.E. Splitt, D.D. Turner, ARM Southern Great Plains Site Observations of the Smoke Pall Associated with the 1998 Central American Fires, *Bull. Amer. Meteor. Soc.*, in press, 2000.

Turner, D.D. and J.E.M. Goldsmith, Twenty-four-hour Raman lidar water vapor measurements during the Atmospheric Radiation Measurement Program's 1996 and 1997 water vapor intensive observation periods, *J. Atmos. and Oceanic Technol.*, 16, 1062-1076, 1999.

Turner, D.D., W.F. Feltz, and R.A. Ferrare, Continuous water vapor profiles from operational ground-based active and passive remote sensors, *Bull. Amer. Meteor. Soc.*, **81**, 1301-1317, 2000.

Turner, D.D., R.A. Ferrare, L.A. Heilman, W.F. Feltz, and T. Tooman, Automated retrievals of aerosol extinction and backscatter coefficient profiles from a Raman lidar, submitted to *J. Appl. Meteor.*, 2000.

Whiteman, D.N., K.D.Evans, B.Demoz, D.O'C.Starr, D.Tobin, W.Feltz, G.J.Jedlovec, S.I. Gutman, G. K. Schwemmer, M. Cadirola, S. H. Melfi, F. J. Schmidlin, "Raman lidar measurements of water vapor and cirrus clouds during the passage of hurricane Bonnie", submitted to *J. Geophys. Res.*, 2000.

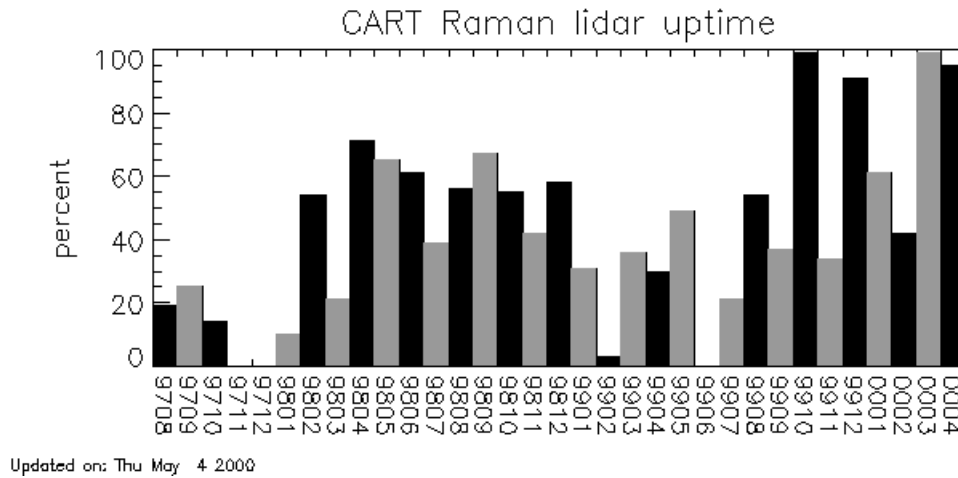


Figure 1. Percentage of run time for CART Raman lidar during each month from August 1997 to May 2000.

Table 1. CART Raman Lidar/AERI+Model Clear-Sky Product Parameters

Measurement	Altitude Range	Vertical Resolution	Nominal Temporal Resolution	Error	Precision	Detection Limit
Aerosol Backscattering (355 nm)	0.060-8 km	78 m	10 min	5-10%	2%	0.0002-0.0004 km-sr ⁻¹
Aerosol Extinction (355 nm)	0.1-8 km	150-500 m	10 min	5-10%	5%	0.02-0.03 km ⁻¹
Aerosol Optical Thickness (355 nm)	-	-	10 min	5% or 0.03	5%	0.03
Water Vapor Mixing Ratio	0.060-8 km (night) 0.060-4 km (day)	78 m	2-10 min	5%	2%	0.002 g/kg
Relative Humidity	0.060-8 km (night) 0.060-4 km (day)	78 m	2-10 min	5%	5%	1%
Precipitable Water Vapor	-	-	10 min	5%	5%	2 mm
Linear Depolarization	1-14 km	39 m	1-10 min	10%	2%	
Temperature (AERI+Model)	0-3 km (AERI) 3-15 (Model)	100 m - 1 km	8 min	1 K	1 K	
Cloud Base Height	0.060-14 km	78 m	1-10 min	78 m	39 m	0.060 km

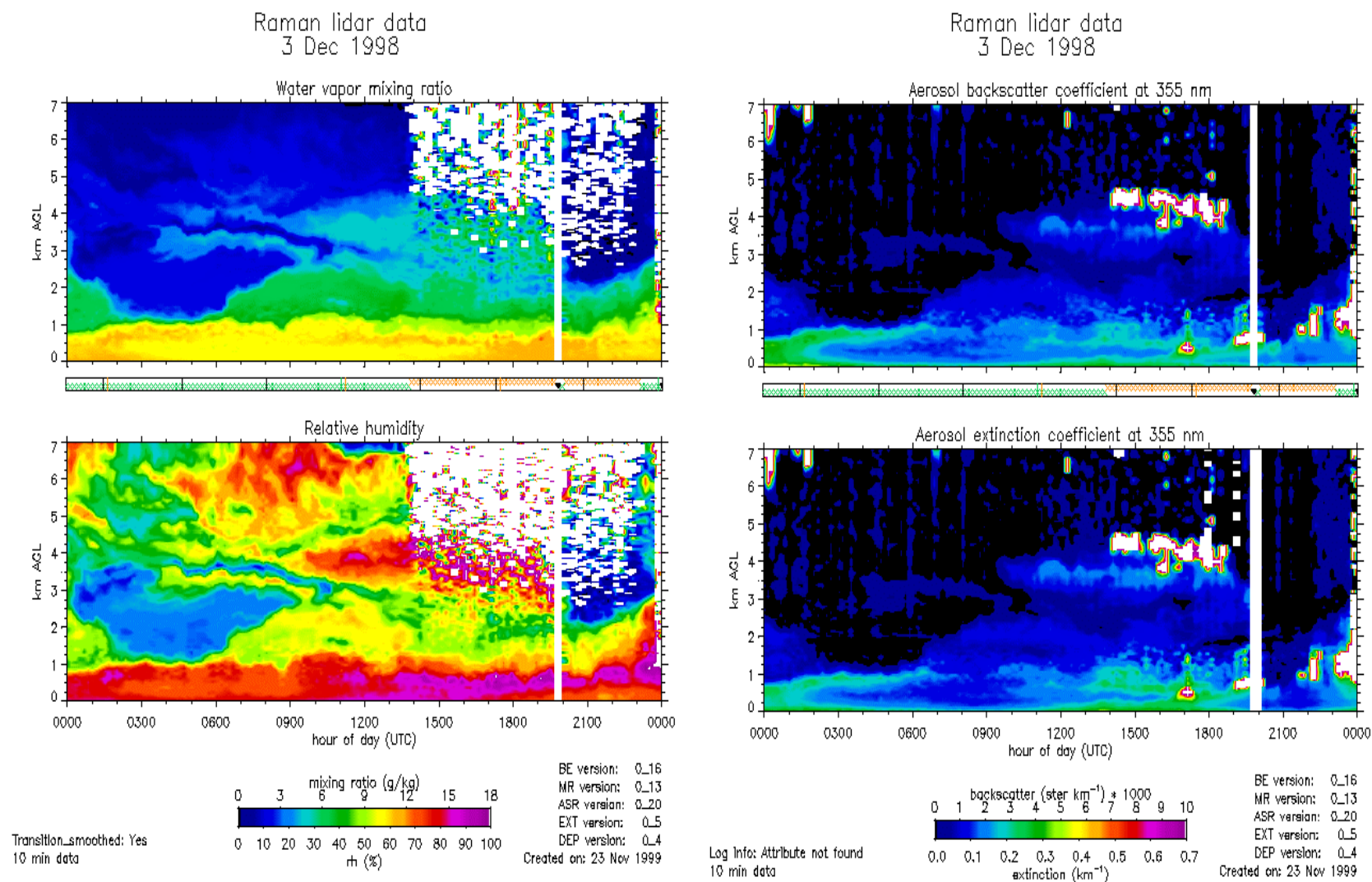


Figure 2. Example of CART Raman lidar water vapor (left) and aerosol (right) “quicklook” images for December 3, 1998.

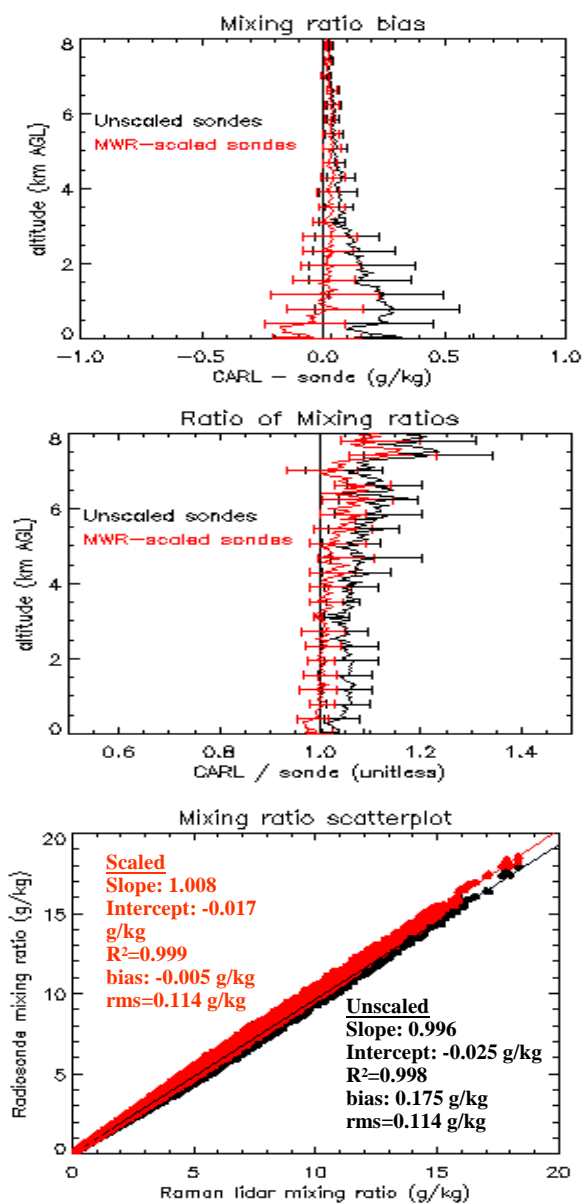


Figure 3. Comparison of CART Raman lidar and Vaisala radiosonde water vapor profile measurements.

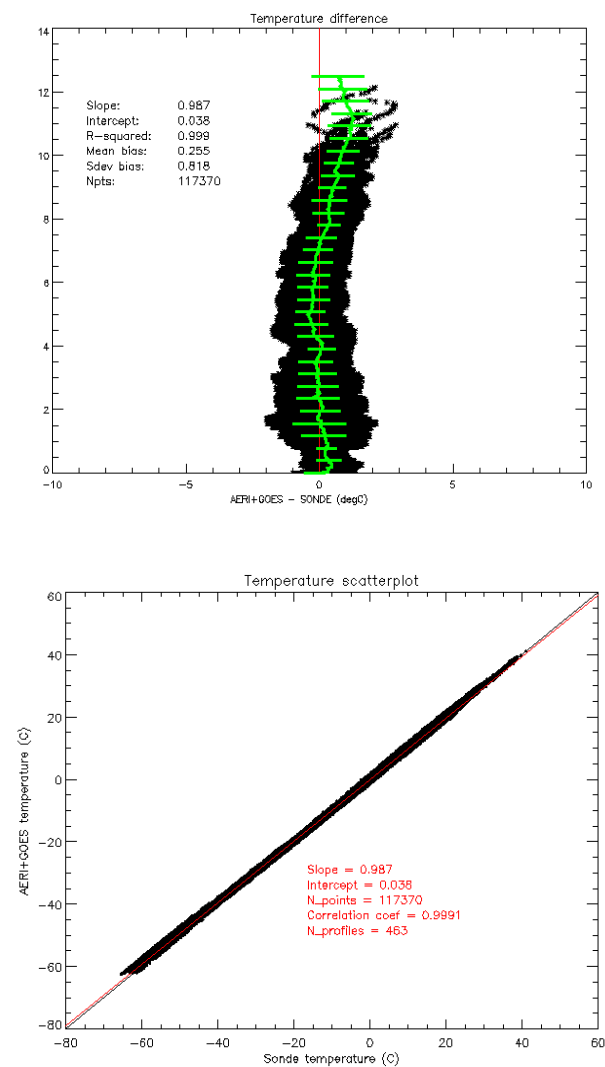


Figure 4. Comparison of AERI+Mode and radiosonde temperature profile measurements.

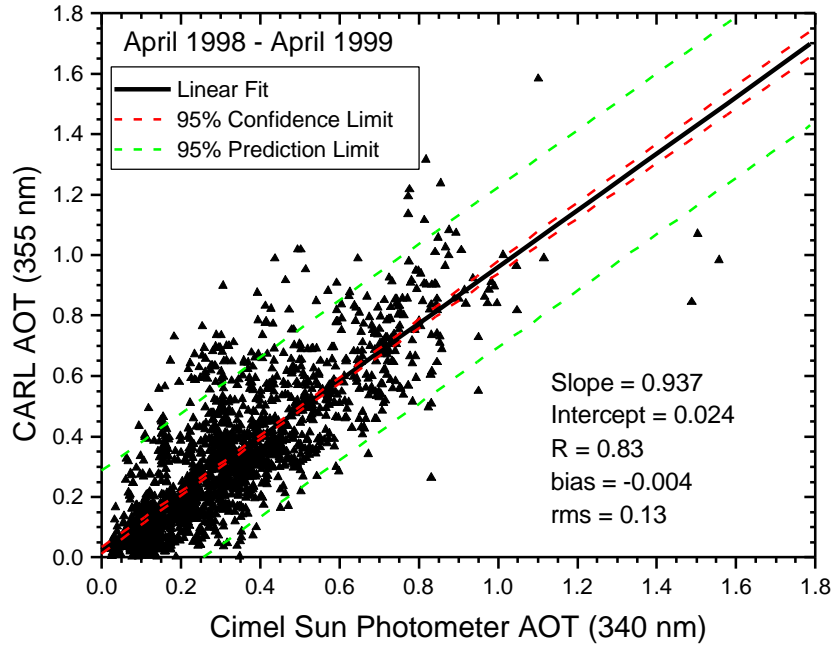


Figure 5. Comparison of AOT measured by Cimel Sun photometer and Raman lidar.

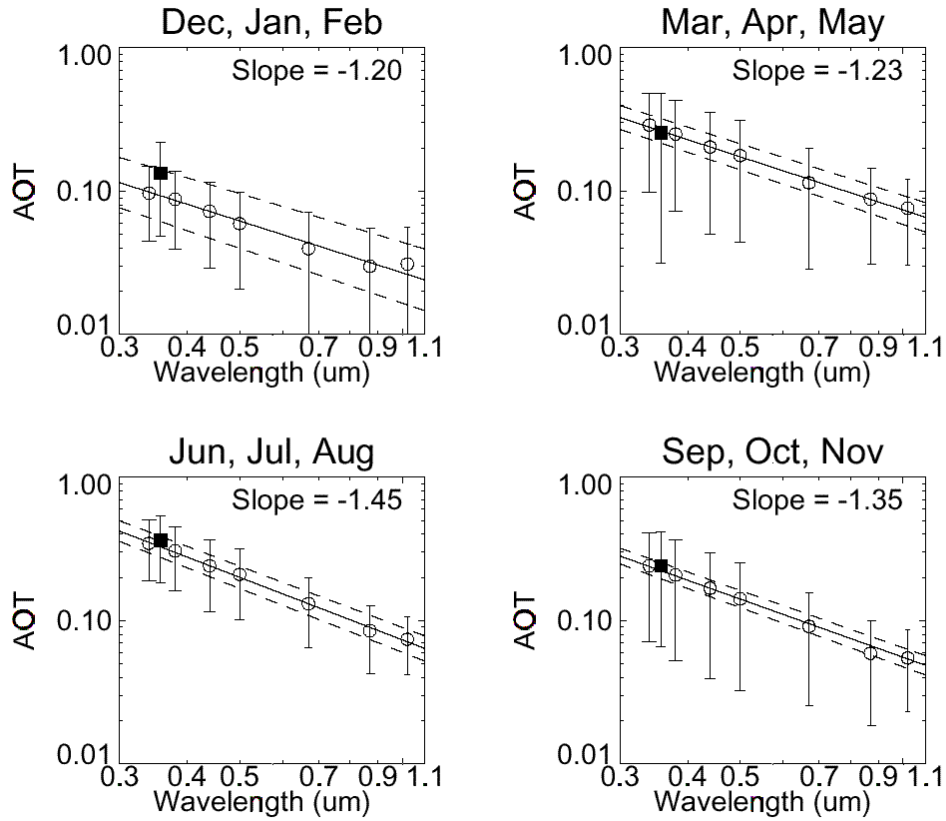


Figure 6. Comparisons of mean AOT from coincident samples from the CIMEL (open circles) and Raman lidar (solid squares) as a function of season. These are log-log plots. There were 225, 571, 562, and 1127 cloud-screened comparisons in the winter, spring, summer, and fall seasons, respectively. The solid lines represent the mean wavelength relationship, while the dotted lines are three times the standard deviation about this mean.

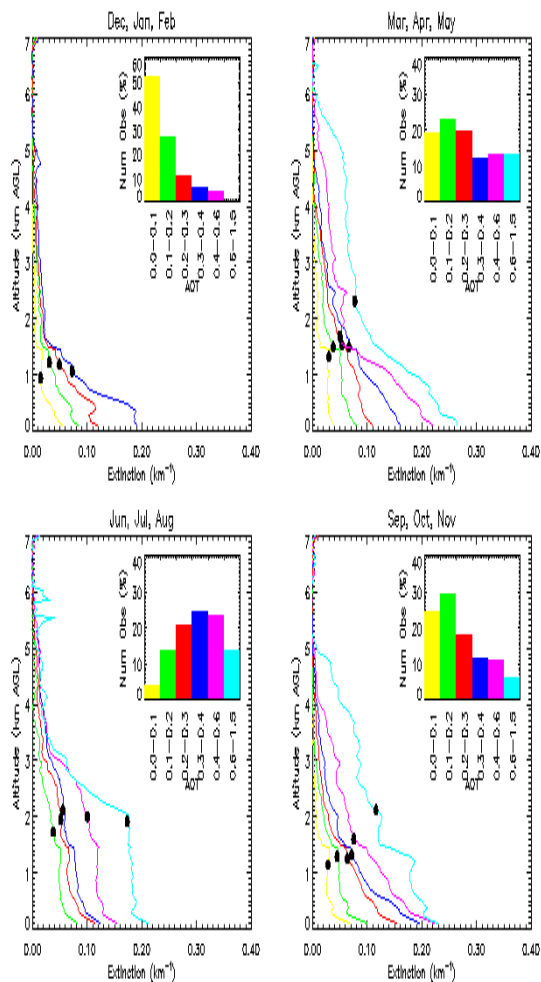


Figure 7. Mean extinction profiles as a function of aerosol optical thickness (AOT) and season for data from April 1998 – January 2000. The inset histograms indicate the distribution of the samples as a function of AOT bin for each season.

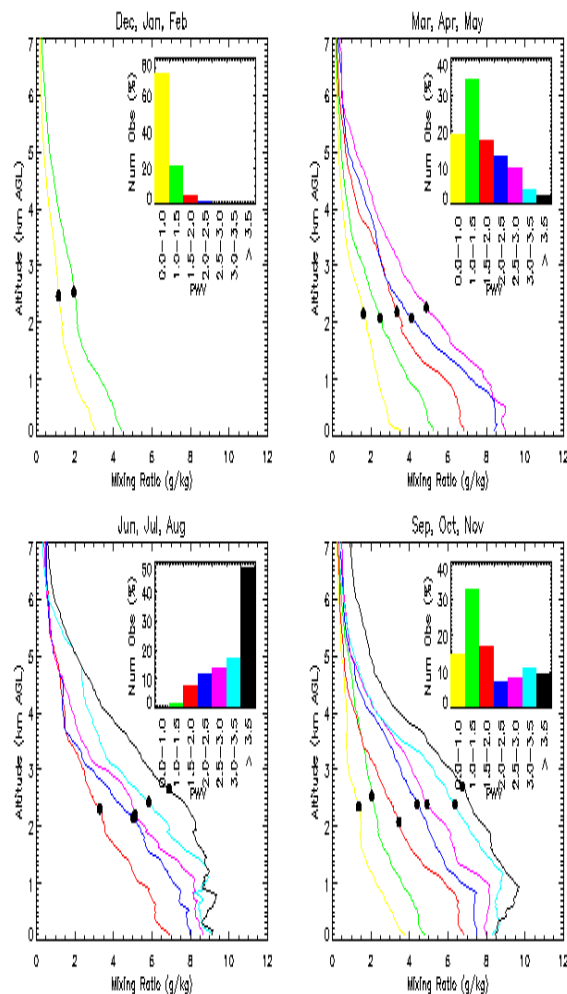


Figure 8. Mean water vapor mixing ratio profiles as a function of season and total precipitable water for data from April 1998 – January 2000. The inset histograms indicate the distribution of the samples as a function of PWV for each season.

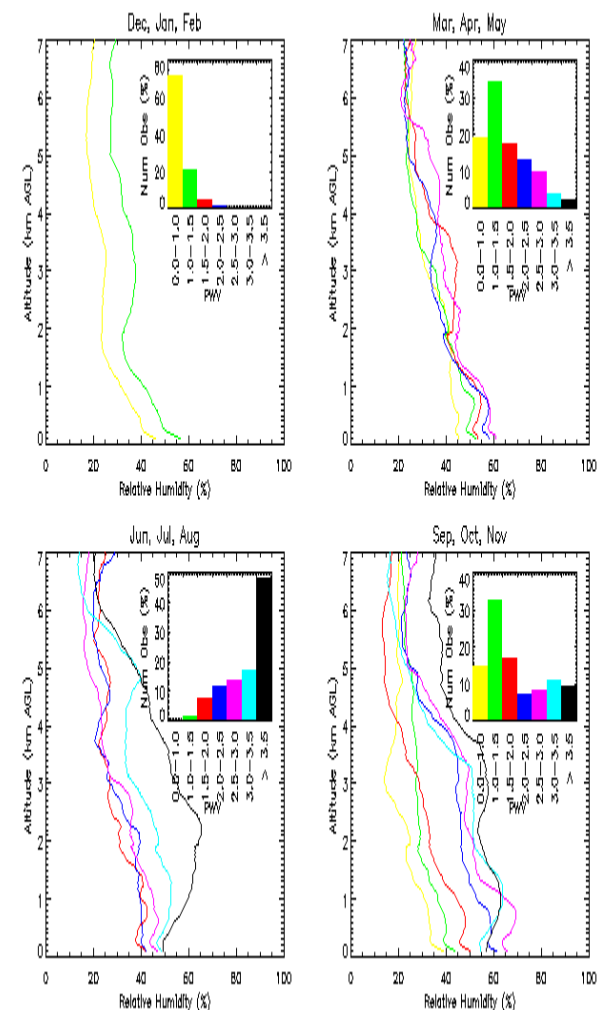


Figure 9. Same as figure 8, except these are mean relative humidity profiles instead of mean mixing ratio profiles.

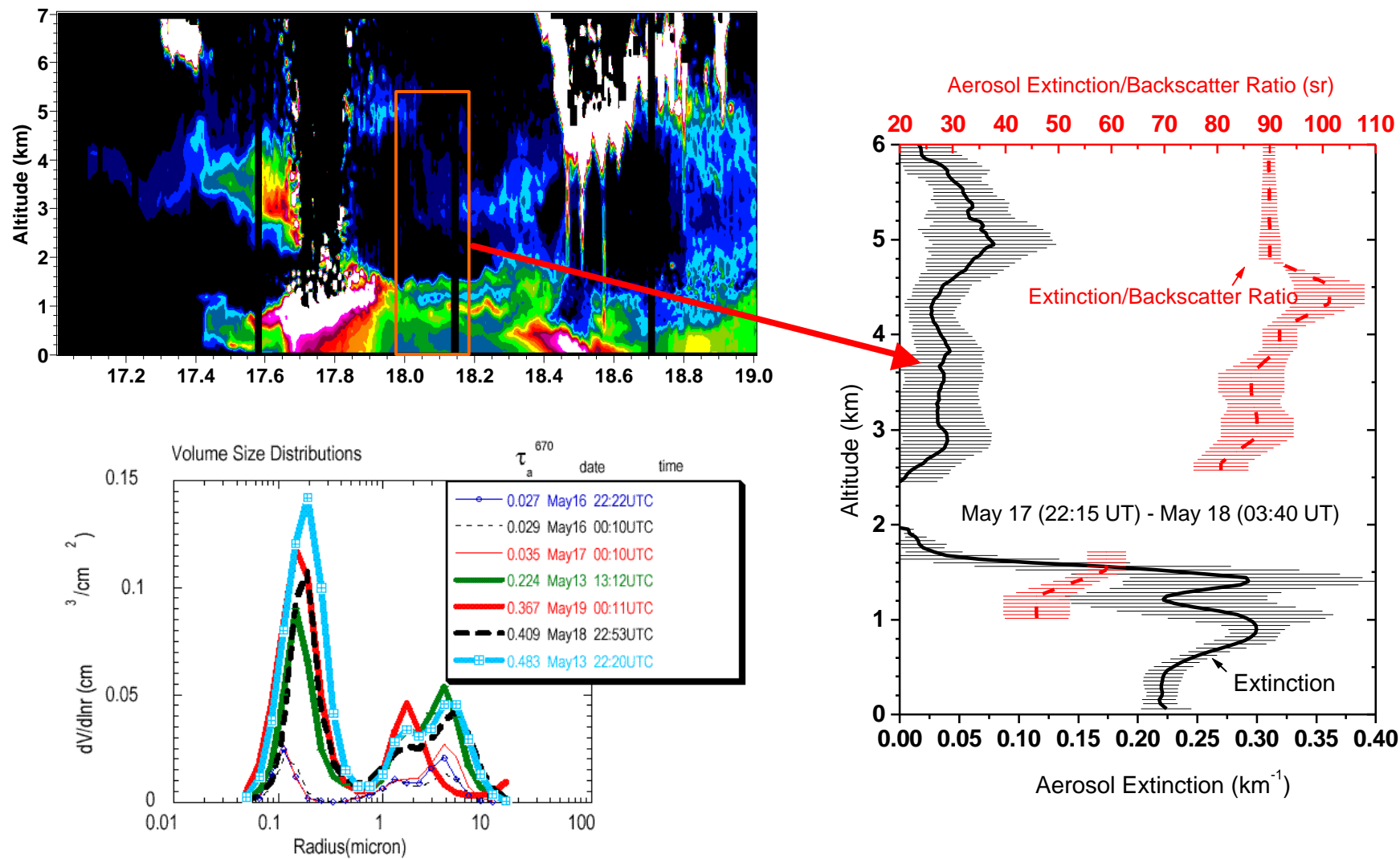


Figure 10 (top left) Image showing CART Raman lidar aerosol extinction profiles acquired on May 17-18, 1998. (right) CART Raman lidar profiles of aerosol extinction and aerosol extinction/backscattering ratio between 22:15 UT May 17 and 03:40 UT May 18. (bottom left) Aerosol volume size distribution derived from Cimel Sun photometer measurements of Sun and sky radiances.

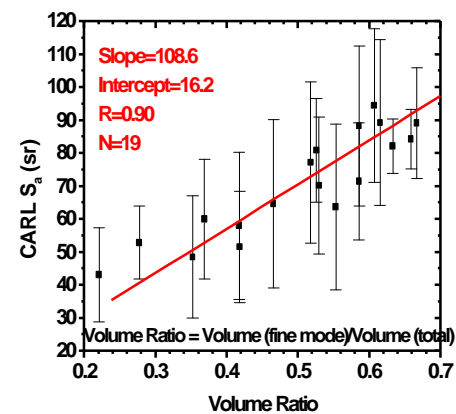
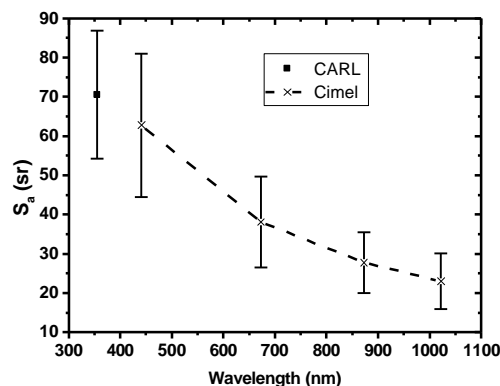
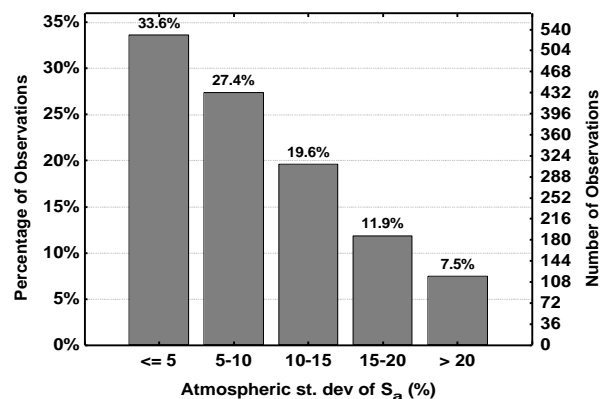
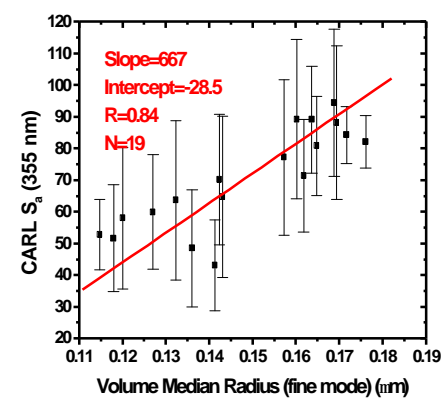
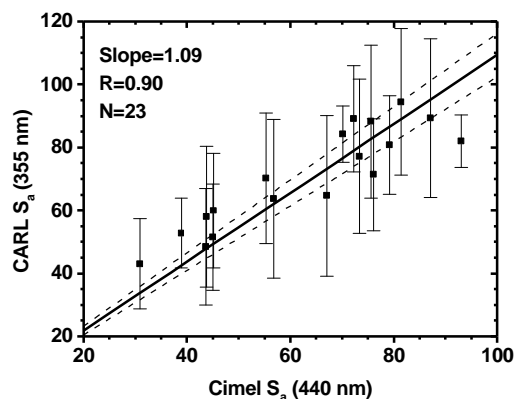
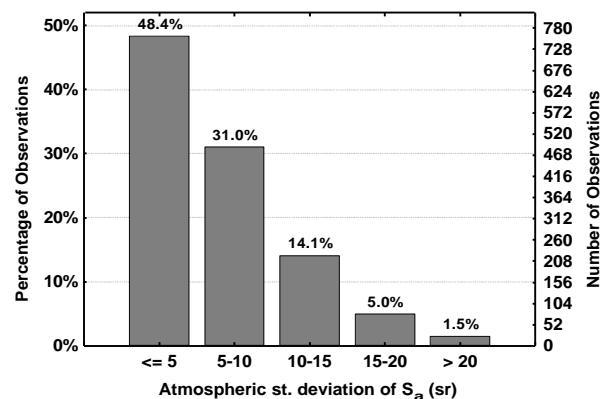


Figure 11. Standard deviation of S_a in a vertical column due to atmospheric variability for CART Raman lidar data acquired between April 1998 and April 1999. Top graph shows standard deviation in steradians and bottom graph shows this as a percentage of the measured S_a

Figure 12. (top) Comparison of S_a measured by CART Raman lidar and derived from Sun and sky radiances measured by Cimel Sun photometer. (bottom) Wavelength dependence of S_a

Figure 13. Comparison of fine mode volume mean radius (top) and volume ratio (bottom) derived by inverting Sun and sky radiances with CART Raman lidar measurements of S_a

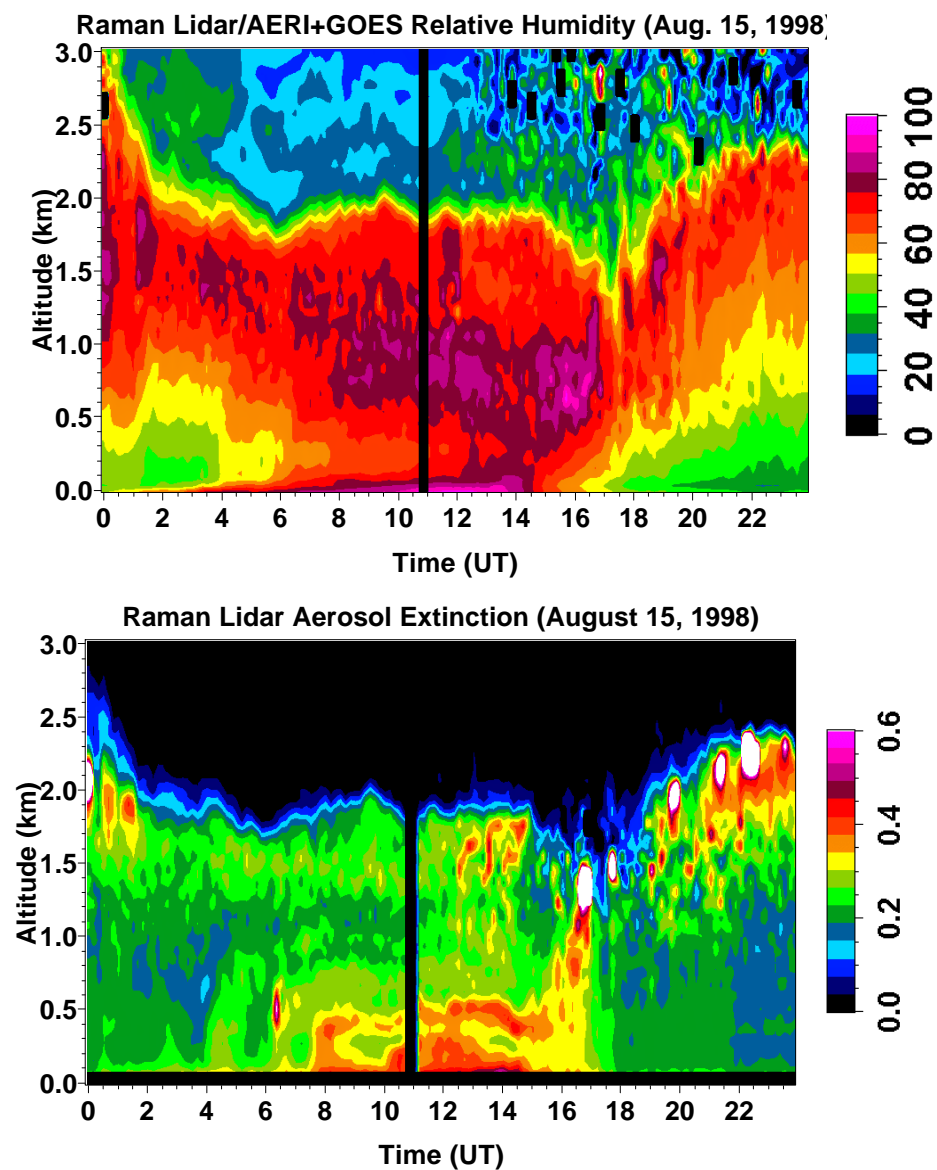


Figure 14. Images showing CART Raman lidar measurements of relative humidity (top) and aerosol extinction (bottom) on August 15, 1998

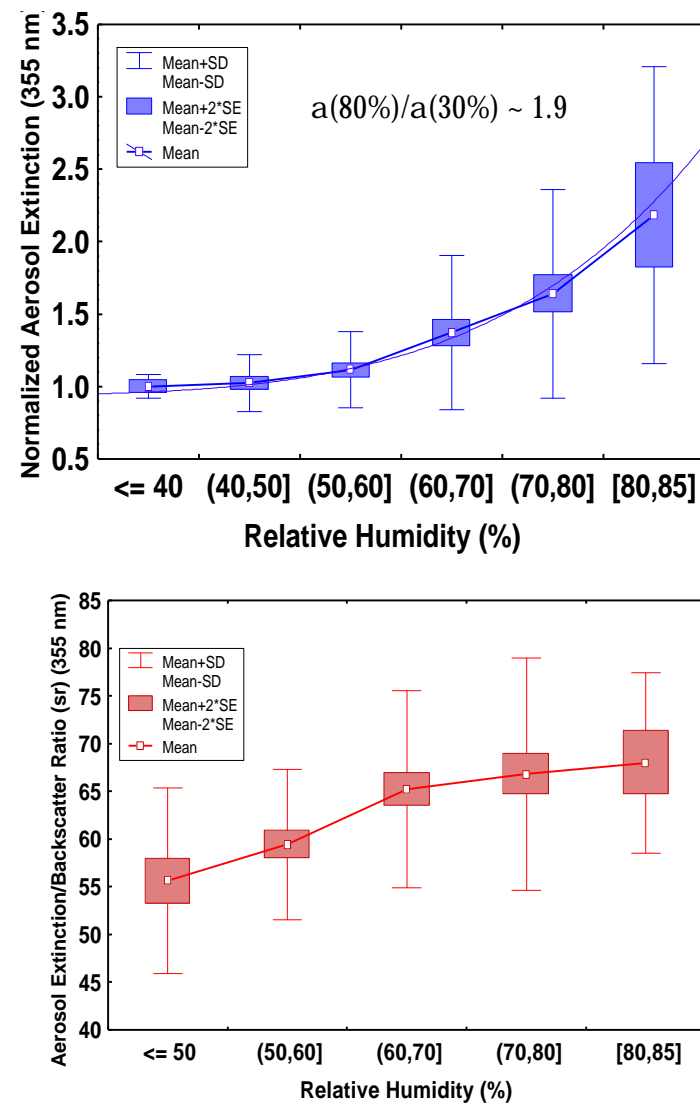


Figure 15. Average distributions of normalized aerosol extinction (top) and aerosol extinction/backscattering ratio (bottom) as a function of relative humidity for cases of hygroscopic aerosol growth near the top of the daytime boundary layer.

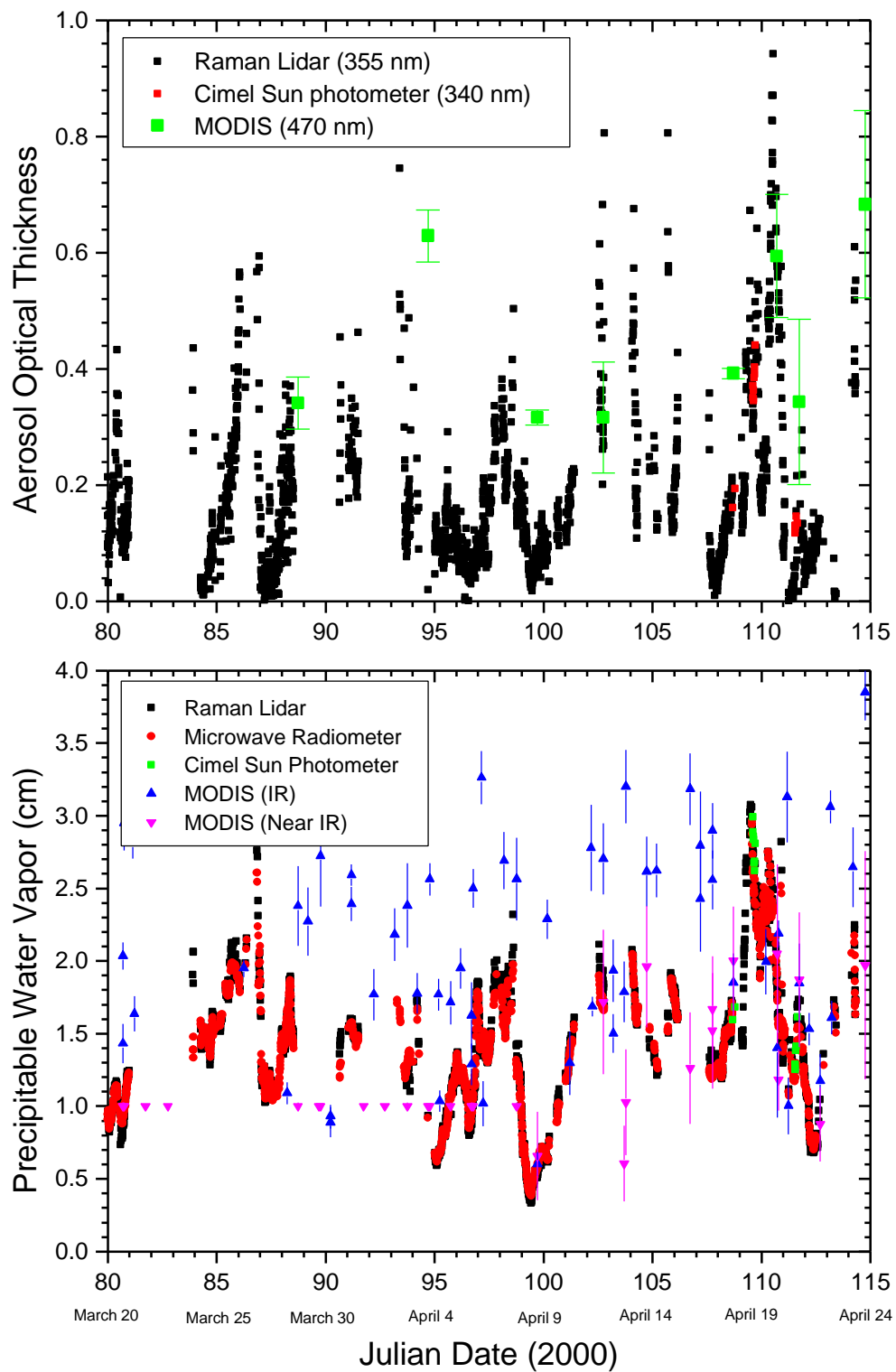


Figure 16 a). Comparisons of AOT measured by Raman lidar and Cimel Sun photometer over the ARM SGP site and MODIS level 2 AOT corrected optical depth for data acquired between March 20 and April 24, 2000. The MODIS data represent an average over a 100 km x 100 km surrounding the SGP site. b). Same as a except for PWV.

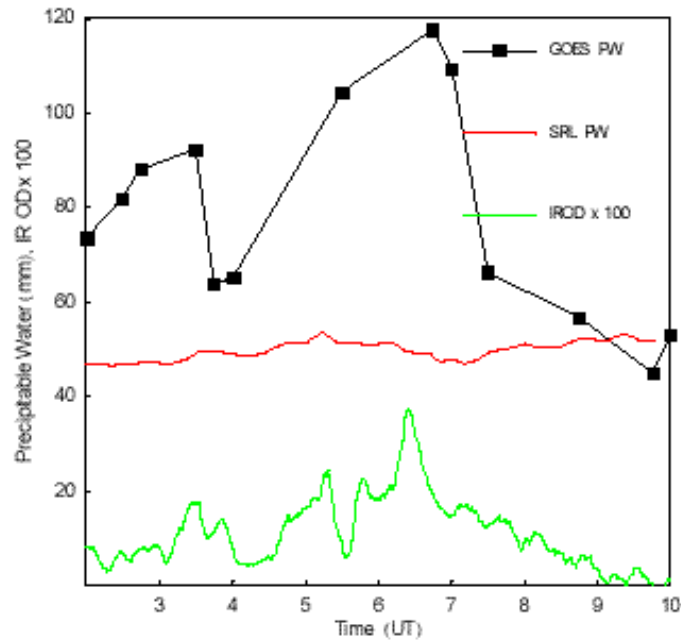


Figure 17. Comparison of Scanning Raman Lidar measurements and retrieved products from GOES satellite. The SRL measurements are from Andros Island, Bahamas in August, 1998. Lidar measurements of cirrus cloud optical depth and total precipitable water (TPW) are shown along with retrieved TPW from GOES satellite using single pixel retrievals of TPW from GOES for the pixel that contained the SRL location. No cloud-clearing was performed in order to study the influence of thin cirrus clouds on satellite radiances. The SRL TPW indicated relatively constant values of TPW during the measurement period while the satellite derived values approached the SRL measurements only for values of cirrus optical depth of approximately 0.005. This study indicated that thin cirrus clouds dominate the radiance viewed by satellites. Also, the bias in TPW due to the presence of cirrus is consistently toward higher values indicating that it is particularly important that satellite cloud-clearing algorithms be able to detect thin cirrus clouds. To the degree that undetected cirrus clouds contaminate the global satellite database of TPW, there should be a consistent high bias in the estimates of global TPW and thus greenhouse feedback.

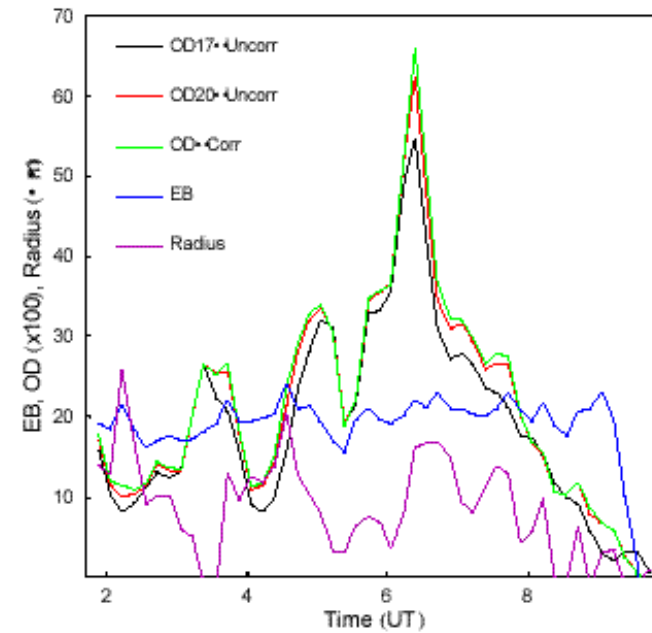


Figure 18. The results of an iterative cirrus cloud retrieval technique are shown. This technique uses the cirrus cloud optical depths calculated at different altitudes and the lidar-derived cloud backscatter coefficient to simultaneously correct for the influence of multiple scattering on cloud optical depth as well as to determine the bulk extinction/backscatter ratio and the radius of the sphere with the same bulk diffraction properties measured in the cloud. The uncorrected optical depth calculations done at 17 km (black) and 20 km (red) are shown to illustrate the influence of the choice of upper reference altitude on the calculated optical depth. The optical depth, after correction for optical depth, is shown in green. Bulk extinction to backscatter ratio is shown in blue and the particle radius is plotted in purple.